Cross-Linked Structures of Nadic-End-Capped Polyimides at 371 °C

April H. Baugher,*,† Matt P. Espe,‡ Jon M. Goetz,‡ Jacob Schaefer,‡ and Ruth H. Pater§

Physics Department, College of William and Mary, Williamsburg, Virginia 23187, Chemistry Department, Washington University, St. Louis, Missouri 63130, and Composite and Polymeric Materials Branch, NASA Langley, Hampton, Virginia 23681

Received October 4, 1996; Revised Manuscript Received June 6, 1997[⊗]

ABSTRACT: The thermally induced cross-linking of nadic-end-capped polyimides has been studied by a variety of spectroscopic techniques. Two nadic-end-capped polyimides were subjected to 371 °C heat treatment for 100 h in order to study cross-linking resulting from elevated temperature. The glass transition temperature of the treated samples increased to greater than 400 °C, indicating that both polyimides underwent extensive chemical changes during heat treatment. ^{13}C spin counts were measured before and after heat treatment by ^{13}C cross-polarization magic angle spinning nuclear magnetic resonance. Electron spin resonance measurements showed an increase in the concentration of stable free radicals in the treated samples. Dynamic nuclear polarization and electron spin resonance results show that two species of free radicals are present in the treated samples; the first is located on the polymer backbone and the second on the cross-linking network that arises from the reaction of the nadic end-capping groups. On the basis of these results, new cross-linking structures of nadic-end-capped polyimides before and after heat treatment at 371 °C are proposed.

Introduction

PMR polyimides are a family of thermosetting polymers prepared from nadic-end-capped imide oligomers by the in-situ polymerization of monomer reactants.[1,2] These polyimides have commercial application as composite matrix resins in a variety of aircraft engine components over the temperature range 232−371 °C.[3] The desirable properties of these systems are mainly attributable to the nadic end-capping group. The cross-linking that occurs through this group controls the thermomechanical properties and the thermooxidative stability of the PMR polyimides. Curiosity about the fate of the nadic end-capping group has motivated many investigations into its cross-linking mechanism and structure in the last three decades. The three predominant cross-linking structures are shown in Figure 1.

In 1971, Lubowitz proposed that the nadic ring undergoes a retro-Diels−Alder reaction to give cyclopentadiene and maleimide followed by their recombination to form the alternating structure I shown in Figure 1.[4] However, the polymer obtained showed little or no unsaturation character, as determined by bromination. To account for the lack of unsaturation, Burns et al. suggested a random vinyl polymerization of cyclopentadiene, maleimide, and nadimide, resulting in structure II in Figure 1.[5] By taking advantage of advances made in nuclear magnetic resonance techniques over the next decade, Wong et al. proposed that cyclopentadiene reacts with the nadic double bond via the Diels−Alder pathway to give a doubly bridged adduct that then reacts with maleimide and nadimide to give a stereochemically and sequentially irregular form shown as structure III in Figure 1.[6] This mechanism has received the support of two independent studies reported recently.[7,8] It should be noted that all of these mechanistic studies were carried out using a model compound, *n*-phenylnadimide, under mild conditions, because fully cured high molecular weight PMR polyimides are intractable and insoluble, precluding the use of solution analytical techniques for characterization. These studies do not rigorously address the subtleties of these systems, and many issues concerning cross-linking remain unclear.

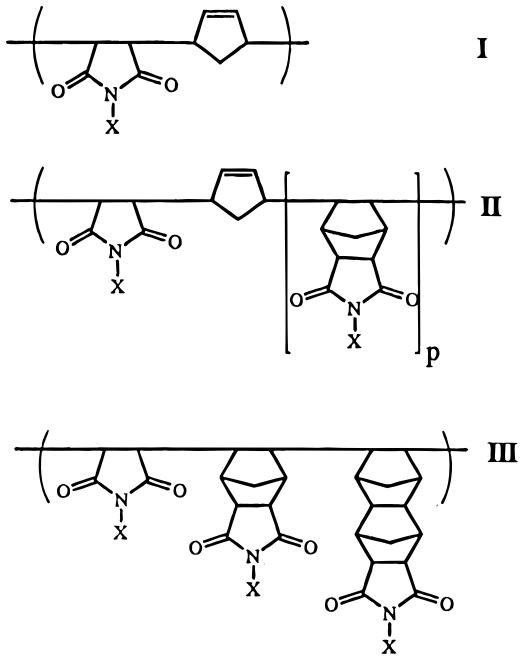

Figure 1. Proposed cross-linking structures for nadic-end-capped polyimides before heat treatment at 371 °C.

Furthermore, recent studies by electron spin resonance[9] and by superconducting quantum interference device magnetometry (SQUID)[10] clearly establish the existence of stable multi-free radical centers in PMR-15 when exposed to 316 and 371 °C temperatures. The proposed structures presented above contain highly strained saturated alicyclic functionalities that cannot account for the presence of these stable radicals.

† College of William and Mary.
‡ Washington University.
§ NASA Langley.
[⊗] Abstract published in *Advance ACS Abstracts,* September 1, 1997.

S0024-9297(96)01480-5 CCC: $14.00

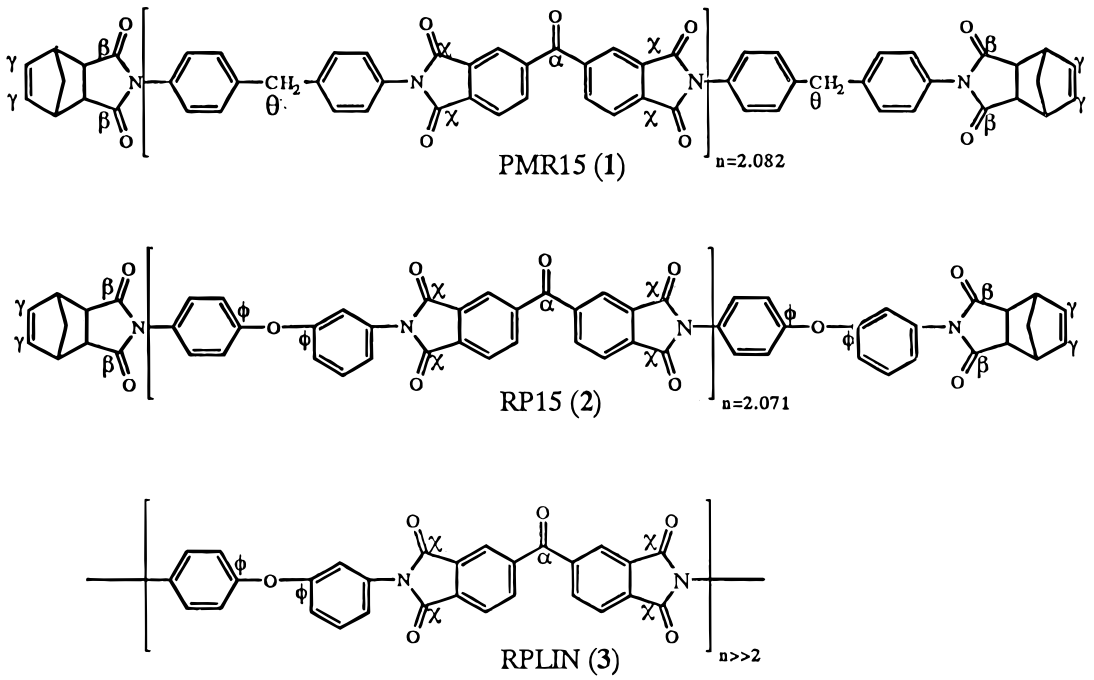

Figure 2. Polyimide oligomers for all three polymers. The Greek letters refer to the chemical shift assignment on the ^{13}C CPMAS NMR spectra below. From here on PMR-15, LaRC RP46 RP15, and LaRC RP46 RPLIN will be referred to by numbers **1**, **2**, and **3**, respectively, as denoted in this figure.

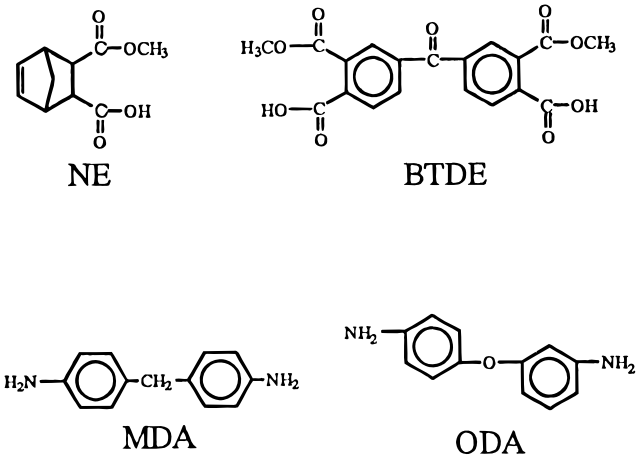

Figure 3. Different monomers used in the synthesis of **1**−**3**. **1** is synthesized through the addition of BTDE, MDA, and NE. **2** is synthesized from BTDE, ODA, and NE. **3** is synthesized from BTDE and ODA only. Cross-linking occurs primarily through the monomer unit NE so only **1** and **2** undergo cross-linking.

To address more rigorously the issues of cross-linking in PMR polyimides under actual use conditions, heat-treated PMR-15, LaRC RP46 (RP15), and its thermoplastic analog RPLIN have been studied using FTIR, ESR, ^{13}C CPMAS NMR, and dynamic nuclear polarization. Based on the results of these experiments, the as-cured and the 371 °C cross-linked structures for nadic end-capped polyimides are proposed.

Experimental Section

Materials. The structures of the three polyimides in their oligomeric form are shown in Figure 2. From here on, PMR-15, RP15, and RPLIN will be referred to by numbers **1**, **2**, and **3**, respectively, as designated in Figure 2. Polymers **1**−**3** were prepared from the monomer reactants shown in Figure 3. Polymer **1** was synthesized in two successive steps from 4,4′-methylenedianiline (MDA), the dimethyl ester of 3,3′,4,4′-benzophenonetetracarboxylic acid (BTDE), and the monomethyl ester of 5-norbornene-2,3-dicarboxylic acid (NE). Polymer **2** underwent a similar synthesis with the monomer reactants 3,4′-oxydianiline ODA, BTDE, and NE. The ratio of the monomer reactants for both polyimides was chosen to give a formula mass of 1500 with the NE groups acting as end caps. The synthesis of **3** consisted of the addition of monomers ODA and BTDE. The cure process for these materials consisted of heating at 316 °C for 1 h under 3300 psi for **1** and **2** and 5555 psi for **3**. Samples of each material were heat treated in air at 371 °C for 50, 75, and 100 h. After heat treament, each sample was ground to a fine powder.

Thermal Characterization. Weight loss during postcure was measured and divided by the sample surface area in order to distinguish between surface degradation and bulk chemical change. Glass transition temperatures were measured by differential scanning calorimetry and by thermomechanical analysis. Differential scanning calorimetry thermograms were recorded using a 20 °C/min heating rate on a DuPont Instruments 910 DSC. A DuPont Instruments thermomechanical analyzer was used with a 5 °C/min heating rate.

FTIR. Infrared spectra were collected with a Nicolet FTIR spectrometer in absorption mode. Each sample was finely ground into a potassium bromide matrix, and 1000 scans were collected for each absorption spectrum.

NMR. Cross-polarization, magic angle spinning ^{13}C NMR spectra were obtained at room temperature at 50.3 MHz on a home built spectrometer, details of which have been described before.[11] Cross-polarization transfer from protons to ^{13}C was made under matched spin lock conditions at 50 kHz with magic angle spinning at 6.25 kHz. Transfer times varied from 1 to 25 ms for the $T_{1\rho}$ experiments. Peak assignments were based on spectra collected for the monomers shown in Figure 3 and the model compound NE−MDA−NE in conjunction with predictions from Chemdraw software by Softcraft. Chemical shifts are given in parts per million downfield from tetramethylsilane using alanine as an external reference.

ESR. ESR measurements were made at room temperature on a Bruker ER200 spectrometer. The microwave frequency was measured with an EIP 628A frequency counter and g values were determined using 1,1-diphenyl-2-picrylhydrazyl (DPPH) as a reference. Spin counts were determined using the stable free radical 1,3-bis(diphenylene)-2-phenylallyl (BDPA) complex with benzene, dispersed in polystyrene.

Dynamic Nuclear Polarization (DNP) ^{13}C CPMAS NMR. The DNP spectrometer operates at 39.4 GHz for electrons and 60 MHz for protons. The microwave irradiation is along the axis of the NMR coil. The microwave cavity is

Table 1. Physical Weight Loss for 1−3, Expressed as the Percent Lost and as the Weight Lost per Surface Area during Heat Treatment, and the Glass Transition Temperatures before and after Heat Treatment

	1			2			3		
hours	T_g (°C)[a]	%[b]	($\times 10^{-3}$ g/cm^2)[c]	T_g (°C)	%	($\times 10^{-3}$ g/cm^2)	T_g (°C)	%	($\times 10^{-3}$ g/cm^2)
0	314	0	0	245	0	0	226	0	0
50	398	6.2	2.2	420	9.5	1.9	302	4.0	0.7
75	408	8.7	2.7	428	14.3	2.7	309	6.7	1.0
100	424	10.7	3.1	432	18.6	3.6	326	7.0	1.2

[a] T_g values have an error of ±5 °C. [b] % weight lost has an error of ±10% of the values shown. [c] Material lost in grams divided by the sample surface area. These values have an error of ±10% of the values shown.

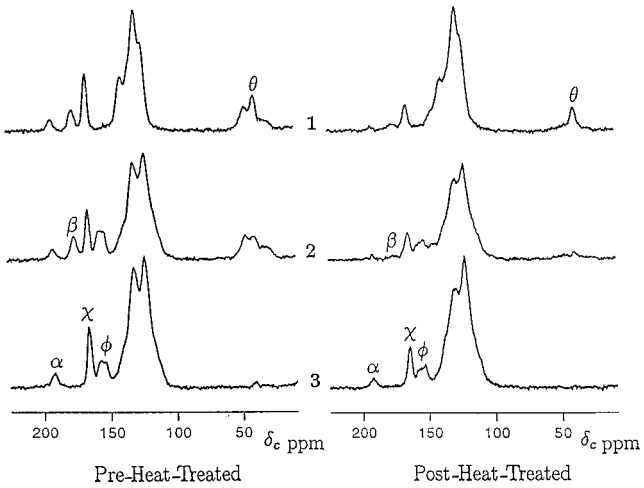

Figure 4. ^{13}C CPMAS NMR spectra before and after heat treatment. The spectra were collected at 200 MHz for protons with a contact time of 1 ms and a recycle time of 3 ms. The Greek letters indicate the chemical shift peak assignments in conjunction with the labels in Figure 2.

formed from the coil and a pneumatically controlled reflector. The static magnetic field was adjusted by an external Helmholtz coil located in the magnetic bore. The home built spectrometer is described in greater detail elsewhere.[12]

The ^{13}C DNP enhancements were obtained using an alternate-block equal-heat sequence. In each pulse sequence, the NMR signal (^{13}C or proton) was acquired twice. In the first half of the experiment, the samples were irradiated with microwaves for 1 s at a frequency near the sum or difference of the electron and nuclear Larmor frequencies before the NMR signal was acquired. In the latter half of the pulse sequence, application of the microwave irradiation was delayed until after signal acquisition. The acquired signal was enhanced by three different methods. First, the proton signal was enhanced and a proton solid echo was acquired. Second, enhancement of the protons was followed by cross-polarization transfer to the ^{13}C and acquisition of the ^{13}C signal. Finally, direct enhancement of the ^{13}C polarization was followed by a $\pi/2$ observation pulse on the carbon channel.

Results

Thermal Characterization. Table 1 lists the physical weight loss during heat treatment and the glass transition temperatures. Similar values for physical weight loss are seen for **1** and **2**, while **3** loses much less. The T_g's of both **1** and **2** undergo a large initial increase after 50 h at 371 °C and then continue to rise more slowly with increasing heat-treatment time. The increase in T_g for **3** is more moderate.

^{13}C CPMAS NMR. Figure 4 depicts the ^{13}C CPMAS NMR spectra of each polyimide before and after heat treatment. All of the chemical shift assignments are designated in Figure 4 in conjunction with the Greek

Table 2. ^{13}C CPMAS NMR Proton $T_{1\rho}$ Values (ms) before and after Heat Treatment As Determined by Fitting the Dependence of the ^{13}C CPMAS NMR Signal Intensity on the Cross-Polarization Transfer Time to Equation 1[a]

	1		2		3	
	0 h	100 h	0 h	100 h	0 h	100 h
α C=C	29[b]	9	20	21	22	29
β C=O	10	10	16	18		
χ C=O	24[b]	11	15	21	15	22
φ ether −O−			15	21	16	25
C=C	11	8	18	15	18	24
aliphatics	7	5	15	*c*		

[a] The $T_{1\rho}$ values listed for the α and χ carbonyls of **1** are apparent values. These two values do not reflect the $T_{1\rho}$ behavior of these functional groups because the α and χ carbonyls are so far removed from protons that cross-polarization transfer occurs very slowly. There is no $T_{1\rho}$ value listed for the aliphatic carbons for **2** because the signal-to-noise was not adequate. The $T_{1\rho}$ values have an error of 3%. [b] Apparent. [c] Inadequate signal-to-noise.

labels in Figure 2. Although all three polymers are structurally similar, there are several differences worth noting. Both cross-linking polymers **1** and **2** have an aliphatic signal around 40 ppm and an imide carbonyl signal at 176 ppm (designated as the β imide C=O), which arise from the end groups. These signals are not seen for **3**. The aliphatic region from **2** is due entirely to carbons in the cross-linking nadic end-capping groups, while the aliphatic region in **1** has contributions from the methylene linkage along the polymer backbone (designated by θ in Figure 2). Both **2** and **3** have peaks at 155 ppm, which are indicative of the ether linkage (designated as φ ether) in the polymer backbone, which is not present in **1**.

To extract quantitative information about the chemical changes occurring during heat treatment using CPMAS NMR, two important magnetic dipolar effects must be considered. The transfer of the magnetic polarization from the proton bath to the carbons is described by the time constant T_{CH}. Concurrently, relaxation of the proton bath occurs with the time constant $T_{1\rho}$. The competition between these two relaxation effects is reflected in the relaxation rates of the different carbon functional groups, and the dependence of the intensity of the ^{13}C signal on the contact time is described in:[13]

$$M(\tau) = M(0)\left(\frac{e^{-\tau/T_{1\rho}} - e^{-\tau/T_{CH}}}{1 - \frac{T_{CH}}{T_{1\rho}}}\right) \quad (1)$$

$M(\tau)$ is the intensity of the ^{13}C NMR signal of each functional group at various cross-polarization contact times τ. By extrapolating to $\tau = 0$, one can find the intensity $M(0)$, which is independent of relaxation effects. Spectra with a range of $M(\tau)$ values were obtained, and the intensities $M(\tau)$ for all of the different carbon functional groups were measured by calculating the integrals of the peaks in the spectra collected with various τ values. The integrals of spinning sidebands were added to those of the corresponding isotropic peaks. These data were fitted to eq 1 by a least χ^2 fitting program to obtain the relaxation parameters $T_{1\rho}$ and $M(0)$. The $M(0)$ values for **1**−**3** are expressed as a percentage of the total intensity of the pre-heat-treated samples and are listed in Table 3. The $T_{1\rho}$ values are listed in Table 2. The $T_{1\rho}$ values for the α and χ carbonyls in heat-treated **1** are denoted as apparent because the isolation of these functional groups from protons causes cross-polarization to occur very slowly

Table 3. ^{13}C CPMAS NMR Spin Counts before and after Heat Treatment As Determined by Fitting the Dependence of the ^{13}C CPMAS NMR Signal Intensity on the Cross-Polarization Transfer Time to Equation 1[a]

	1			**2**			**3**		
	0 h	100 h	Δ	0 h	100 h	Δ	0 h	100 h	Δ
α C=O	2.4	1.7	29	1.8	1.1	39	2.8	2.3	18
β C=O	4.8	1.6	67	3.0	1.1	63			
χ C=O	9.8	6.2	37	10	6.2	41	16	8.7	46
φ ether −O−				7.8	4.9	37	8.0	7.7	4.2
C=C	64	57	11	63	45	28	73	69	5.5
aliphatics	19	7.9	58	14	4.8	66			
total	100	74	26	100	63	37	100	87	13

[a] The spin counts for the heat-treated samples are given as a percentage of the totals for the pre-heat-treated sample, and the percentage change during heat treatment is given. The loss of total ^{13}C CPMAS NMR signal seen for the heat-treated samples is attributed to strong dipolar coupling between the ^{1}H and ^{13}C nuclei and the unpaired electrons. The ^{13}C CPMAS NMR spin counts have an error of 3%.

Table 4. Relative Intensities of FTIR Absorption Bands for the Amide and the Imide Resonances before and after Heat Treatment[a]

	3485 cm^{-1} (OH amide)		3300 cm^{-1} (NH amide)		1779 cm^{-1} (χ and β C=O imide)	
	0 h	100 h	0 h	100 h	0 h	100 h
1	1.9	0.7	0.5	1.1	0.5	0.5
2	2.6	0.3	0.7	1.1	0.4	0.4
3	1.1	0.5	1.2	0.9	0.3	0.5

[a] Each intensity is normalized to the α carbonyl peak at 1610 cm^{-1}, which is not expected to change. The relative intensities have an error of 5%.

Table 5. ESR Parameters before and after Heat Treatment[a]

	g values		line widths (*G*)		spins/g (×10^{18})	
	0 h	100 h	0 h	100 h	0 h	100 h
1	2.0033	2.0029	6.2	5.4	0.2	14
2	2.0035	2.0030	6.2	5.1	0.4	15
3	2.0032	2.0031	5.5	4.7	1.4	7.2

[a] The *g* values were measured using DPPH as a reference, and spin counts were determined using a BPDA complex with benzene, dispersed in polystyrene. The line widths have an error of 5%, and the spin counts have an error of 4%.

so that the relaxation behavior of these magnetization intensities at long times does not reflect the $T_{1\rho}$ behavior. Additionally, the $T_{1\rho}$ value for the aliphatic carbons in heat-treated **2** is not reported because the signal-to-noise ratio was inadequate to fit the relaxation behavior.

FTIR. Table 4 shows peak integrals of the FTIR resonances for the imide carbonyl (β and χ labels in Figure 2) at 1779 cm^{-1}, the amide −OH group at 3485 cm^{-1}, and the amide −NH group at 3300 cm^{-1}. The amide group is not shown in the oligomers shown in Figure 2 but results from incomplete ring closure of the imide ring by the χ imide carbonyls. The integrals were normalized to the integral of the α carbonyl resonance at 1610 cm^{-1}, which is not expected to change with heat treatment. This assumption is consistent with NMR results discussed below.

ESR. The ESR parameters for all three polymers before and after heat treatment are given in Table 5. The *g* values and line widths of the free radicals are indicative of carbon-based π-radicals. The free radicals present before heat treatment result from curing at 316 °C. After heat treatment, there is a substantial increase in the number of free radicals for all three polymers, but the increase is much larger for **1** and **2**, which undergo cross-linking. Similar increases are reported by Ahn et al. in their study of **1**.[9]

1 and **2** have approximately twice as many radicals per gram as **3** after heat treatment. By considering the oligomers shown in Figure 2, it can be calculated that after heat treatment, **1**−**3** have 3.7, 3.5, and 1.2 free radicals per hundred oligomeric units, respectively. These numbers are in good agreement with those taken recently by SQUID measurements.[10] [**3** is a substantially longer oligomer than **1** and **2**. In order to make a relevant comparison between the radicals/oligomer for the three polymers, the calculation for **3** used two repeat units.]

DNP. Figure 5 shows ^{13}C CPMAS NMR spectra for heat-treated **2** collected at 15.1 MHz with and without microwave irradiation. The bottom spectrum is a standard CPMAS spectrum. The difference spectrum in the middle compares the bottom CPMAS spectrum with that obtained after 1 s of microwave irradiation applied at the difference of the electron and proton Larmor frequencies, followed by cross-polarization from the protons to the carbons. The difference spectrum in the middle shows that the ^{13}C spectrum is uniformly enhanced by the microwave irradiation independent of the chemical shift. The top spectrum is obtained after the application of microwave irradiation for 1 s at the difference of the electron and carbon Larmor frequencies, followed by a $\pi/2$ pulse on the carbon channel. The top spectrum also shows uniform enhancement of the different carbon functional groups. Similar results were seen for heat-treated **1** and **3**, for which the spectra are not shown.

DNP enhancement curves for **2** and **3** are shown in Figure 6. The magnitude of the enhancement, ϵ, is measured by comparing the amplitudes of the proton solid echo with (A_{PE}) and without (A_P) microwave irradiation.

$$\epsilon = \left(\frac{A_{PE}}{A_P}\right) - 1 \qquad (2)$$

In Figure 6, the proton enhancement is plotted versus the difference between the microwave frequency and the resonance frequency of the unpaired electrons, $(\omega - \omega_e)/2\pi$. The maximum enhancement of the proton solid echo amplitude gives $\epsilon = 0.9$, 0.7, and 0.4 for **1**−**3**, respectively. The enhancement curves for **2** and **3** in Figure 6 have maximum positive and negative enhancements at $(\omega + \omega_e)/2\pi = 60$ MHz and $(\omega - \omega_e)/2\pi = -60$ MHz. There are also contributions to the curve near $|\omega \pm \omega_e|/2\pi = \pm 25$ MHz. The enhancement curve for **1** is quite similar to **2**.

Discussion

Thermal Characterization. Before heat treatment, polymer **2** has a substantially lower T_g than **1**. This is attributed to a lower degree of cross-linking in **2** than **1** when subjected to the same cure conditions. Thus **2** is only partially cross-linked before heat treatment,

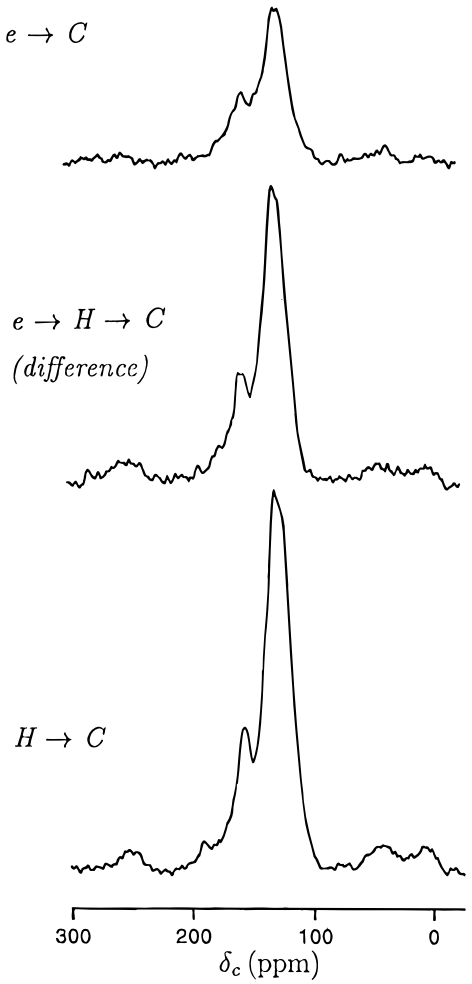

Figure 5. 15.1 MHz CPMAS ^{13}C NMR spectra of heat-treated **2** with and without microwave irradiation. The bottom spectrum is attained using standard CPMAS (H → C) techniques. The middle spectrum is the difference between the CPMAS at the bottom and the DNP-enhanced spectrum collected after microwave irradiation for 1 s at the difference of the electron and proton Larmor frequencies (e → H). The proton polarization was then transferred by CPMAS to the carbons before the spectrum was collected. The top spectrum is the DNP-enhanced spectrum collected after microwaves were applied for 1 s at the difference of the electron and carbon Larmor frequencies (e → C), followed by a $\pi/2$ pulse on the carbon channel. All three spectra used a spinning speed of 1.86 kHz and 10 240 scans.

while **1** is more fully cross-linked. After heat treatment, the T_g values for **1** and **2** increase rapidly to greater than 410 °C. Continued cross-linking cannot account for this increase, which indicates that supplemental chemical changes occur during heat treatment in the cross-linking samples.

^{13}C CPMAS NMR. Table 3 shows that there is a decrease in ^{13}C signal intensity for all three polymers after heating. The signal loss after heat treatment is attributed to strong dipolar coupling between the ^1H and ^{13}C nuclei and the free radicals, which are in close proximity (less than 20 Å). Heat-treated **1** and **2** lose more signal than **3**, which agrees with the higher free radical spin counts for **1** and **2** shown by the ESR results. By comparing the change in ^{13}C NMR spin counts in Table 3 for each functional group with the change in the total spin count for the heat-treated polymer, it is clear that **1** and **2** undergo significant chemical changes during heat treatment. The spin counts for heat-treated **1** and **2** from the β imide carbonyls and the aliphatic carbons on the end groups undergo a substantial reduction, while the the C=C

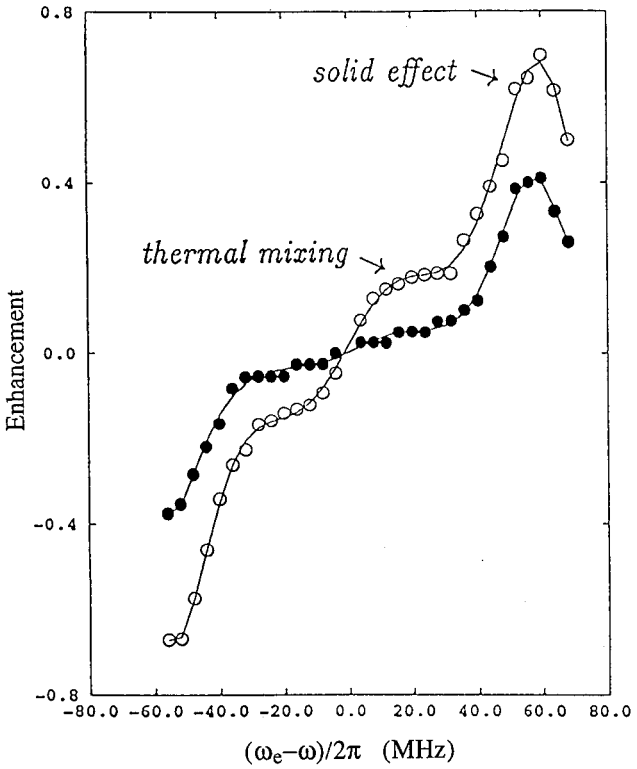

Figure 6. Magnetic field dependence of the proton DNP enhancement obtained from **2** (open circles) and **3** (closed circles) at room temperature. The enhancement was determined by comparing proton Hahn echoes measured with and without microwave irradiation. The lines drawn through the points are a tenth-order spline fit.

NMR spin counts decrease less. This suggests that the aliphatic carbons of the end group are converted to C=C carbons through dehydrogenation, or their signals are lost because of their proximity to the free radical.

In Figure 4, the aliphatic intensity remaining in **1** after heat treatment is attributed to the methylene linkages in the backbone of the polymer. Both **1** and **2** have the same nadic end cap, and **2** loses almost all of its aliphatic intensity on heat treatment, so the same effect is expected in **1**. The result that the methylene linkage survives the heat treatment contradicts previous publications[14] in which conversion of this group to a carbonyl was anticipated. If the group did undergo this conversion, the resulting carbonyl would have a chemical shift like the α C=O, but little change in this peak is seen.

Little change is seen for **3** during heat treatment. Of special interest is the small change in the signal from the θ ether linkage. Previous studies predicted cleavage of the ether linkage on high-temperature heat treatment,[15] but no evidence for this was seen. Similarly, the ether linkage in **2** changes little with heat treatment.

ESR. The ESR spectra from free radicals formed in the three polymers before and after heat treatment are characteristic of π-radicals. The relatively narrow line widths indicate that the unpaired electrons are isolated and delocalized. The free radicals produced in **3** during heat treatment are located in the backbone, because **3** does not have cross-linking groups. Similar free radicals should be generated in **1** and **2**. Since there are fewer backbone units per gram in these two polymers, there should be a lower concentration of backbone-based free radicals. The additional ESR intensity seen in **1** and **2** after heat treatment indicates that a second species of free radical is present. A previous study conducted by

Table 6. Calculated ^{13}C CPMAS NMR Spin Counts (ppm) before Heat Treatment for 1 and 2 for the Aliphatic and C=C Functional Groups Expressed as a Percentage of the Total Number of Carbons[a]

	1					**2**				
	o	I	II ($n = 4$)	II ($n = 9$)	III	o	I	II ($n = 4$)	II ($n = 9$)	III
C=C	70.3	70.3	67.2	66.7	66.0	66.1	66.1	62.6	62.1	61.7
aliphatics	14.3	14.3	17.4	17.8	18.3	11.1	11.1	14.7	15.1	15.5

[a] I−III refer to the proposed cross-linking structures shown in Figure 1 and o is for the oligomer spin counts.

Ahn et al. found an anomaly in the temperature dependence of the ESR intensity in treated **1**, which was attributed to the presence of a second free radical species.[9,10] This free radical is created in the cross-linking network formed from the nadic end caps.

FTIR. The studies of Ahn et al.[9] propose that the low bond energy of the imide carbon−nitrogen bond in the backbone of all three polymers makes this the most likely site for homolytic bond cleavage, and thus the origin of the free radical in the polymer backbone. The FTIR results discussed above and in Table 4 refute this. No change is seen in the integral of the imide FTIR resonances. However, there is a strong signal seen for the amide −OH resonance around 3450 cm^{-1}, as shown in Table 4. This resonance occurs when polymerization of the monomer reactants that form the backbone of the polymer does not result in ring closure to form the imide ring. After heat treatment, this peak is depleted, but the concentration of the imide carbonyl changes little. This suggests that abstraction of the −OH group from the unclosed amide ring gives rise to the free radical in the backbone of the polymer. The free radical found in the cross-linking network of **1** and **2** will not necessarily have the same origin, because the chemical reaction that results in the addition of the nadic end caps is kinetically more favorable than the reaction that occurs in the polymer backbone.

DNP. The similarity of the ^{13}C CPMAS NMR spectra with and without DNP enhancements shown in Figure 5 has several implications. Because the polarization enhancement is a dipolar effect, the nuclei closest to the electrons should have the largest enhancement. However, in enhancing the proton signal, rapid spin diffusion of the proton bath results in nearly equal enhancement for all of the protons, resulting in equal enhancement of all of the ^{13}C signals on cross-polarization. The ^{13}C nuclei do not undergo rapid spin diffusion, so the equivalent enhancement of the spectrum after direct enhancement of the carbon nuclei indicates that all of the carbons are comparably placed to an unpaired electron. This is not counting the lost intensity from carbons which participate in the intramolecular delocalization of the electron.

Since the enhancement maxima and minima seen in Figure 6 occur at $|\omega \pm \omega_e|/2\pi = 60$ MHz for all three polymers, the dominant mechanism for DNP enhancement is the solid effect.[16] This indicates that the unpaired electrons generated during heat treatment are stationary and mostly well separated. The proton and ^{13}C enhancement occurs predominantly by dipolar coupling to the unpaired electrons. The shoulders on the enhancement curves at $|\omega \pm \omega_e|/2\pi = 25$ MHz arise from the thermal mixing mechanism.[16] This enhancement occurs for electrons that are close enough to undergo weak exchange interactions. The ratio of thermal mixing to solid effect enhancement is similar for **1** and **2** but is much less for **3**. This is consistent with the lower radical concentration in **3**, which reduces the likelihood of electron−electron interaction.

In the enhancement curves for **1** and **2**, $\epsilon = 0$ does not occur at ω_e. This asymmetry indicates the presence of an Overhauser enhancement at ω_e. This is not seen for **3**, so the free radicals that give rise to the Overhauser enhancement are assumed to be in the cross-linking network formed by the nadic end caps. The positive Overhauser enhancement results from modulation of the electron−proton isotropic hyperfine coupling at or near the microwave frequency of 40 GHz. The protons that experience this enhancement have a scalar hyperfine coupling to the unpaired electron, as well as a reduced paramagnetic shift. Protons bonded to a carbon that has as little as 1% of the unpaired spin density will be shifted outside the bandwidth of the experiment and will not be observed.[17] However, rapid flipping of the electron spins will reduce the proton paramagnetic shift. This flipping occurs for electrons that undergo strong electron−electron exchange interactions.[18] The Overhauser enhancement is small compared to the other mechanisms of DNP enhancement, implying that only a small fraction of the conjugated structures formed from the nadic end caps hosts more than one free radical.

Proposed Structure before Heat Treatment. Table 6 shows calculated ^{13}C CPMAS NMR spin counts for the cross-linking polymers taking into account the three proposed cross-linking structures shown in Figure 1. The difference between the three proposed structures is most apparent in the degree of unsaturation in the cross-linking structures, as shown in Table 6. For structure I, the olefin bond in the end cap gives the highest C=C percentage and the lowest aliphatic percentage. The degree of unsaturation for structure II depends on the value of p from Figure 1. For a p greater than 1, the C=C percentage is lower than in I and the aliphatic percentage is higher. Structure III does not have the olefin bond, so the C=C spin count percentage is the lowest and the aliphatic percentage is the highest.

The best agreement for **1** arises from the calculation using structure II with an n around 9 or structure III as the mechanism for cross-linking. For **2**, which is only partially cross-linked, the spin counts of the oligomer have to be considered in addition to the various cross-linking mechanisms. Since the oligomer of **2** has a high C=C spin count due to the olefin bond in the end cap, the experimental C=C spin count for **2** will be high. This suggests that the correct cross-linking structure for **2** is also structure II with a high value of n or structure III.

After Heat Treatment. The ESR results indicate that the stable free radicals in the cross-linking groups are π-radicals that are delocalized over highly conjugated chains. The conjugation is extensive enough to allow some free radicals to move around through the chains, which gives rise to the Overhauser effect seen by DNP. Thus the resulting heat-treated structure for **1** and **2** must be able to stabilize the free radicals in the cross-linking network. The ^{13}C NMR spin counts show a decrease in the aliphatic spin counts and an increase in the C=C spin counts, suggesting an increase in conjugation of the cross-linking network. By considering the structures shown in Figure 1, it can be seen that when the cross-linking groups become conjugated,

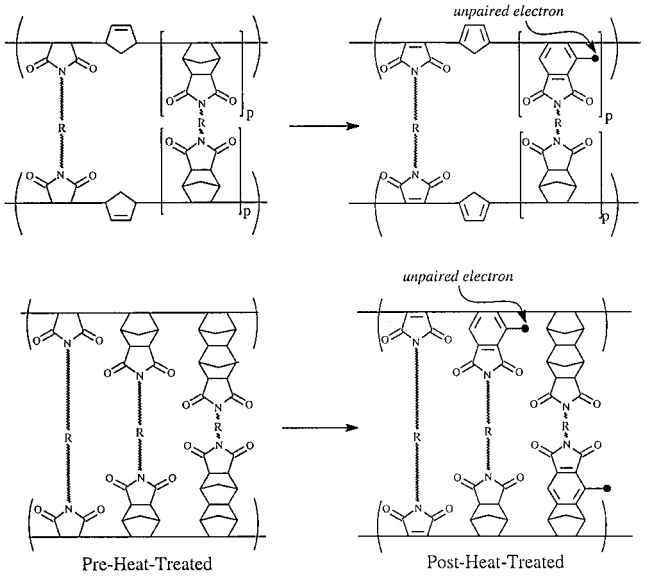

Figure 7. Proposed ideal structures for the nadic end-capping groups in **1** and **2** based on cross-linking structurs **II** (top) and **III** (bottom) of Figure 1 before heat treatment (left) and after heat treatment (right). These structures result from breaking the aliphatic bridge in the nadic end cap shown in the pre-heat-treated structures at the top and bottom of the figure. Abstraction of hydrogen gives the conjugated post-heat-treated structure shown.

both II and III form highly aromatic structures whereas I forms an olefin structure. Since aromatic/benzylic free radicals are more stable than olefin free radicals, this suggests that II and III are better able to stabilize the free radicals resulting from the heat treatment of polymers **1** and **2**. This is in agreement with the prediction made for the pre-heat-treated samples from the ^{13}C NMR spin counts above.

The aromatic structures formed from II and III after heat treatment are shown in Figure 7. These structures result from breaking the aliphatic bridge in the nadic end cap shown in the pre-heat-treated structures at the left of each figure. Abstraction of a hydrogen free radical gives the conjugated post-heat-treated structure shown.

Conclusions

The formation of two different free radical species in **1** and **2** after heat treatment at 371 °C has been proposed. The first species of free radical seen in **1**−**3** is found in the backbone of the polymer and is present in all three polymers before heat treatment. The second species of free radical is only present in **1** and **2** after heat treatment. This free radical is delocalized in the conjugated chains of the cross-linking structures.

Cross-linking structures have been proposed for **1** and **2** before heat treatment, which are in agreement with previously published results. The structures proposed for **1** and **2** after heat treatment account for the presence of stable delocalized π-radicals in the cross-linking endcaps. We have combined powerful analytical techniques—solid state NMR, DNP, ESR, and FTIR—to provide previously unavailable insight into the cross-linking structure of nadic-end-capped polyimides.

References and Notes

(1) Lubowitz, H. R. U.S. Patent 3,528,950, 1970.
(2) Serefini, T. T.; Delvigs, P.; Lightsey, G. R. *J. Appl. Polym. Sci.* **1972**, *16*, 905.
(3) Pater, R. H. *SAMPE J.* **1994**, *30*, 29.
(4) Lubowitz, H. R. *ACS Org. Coat. Plast. Chem.* **1971**, *31*, 560.
(5) Burns, E. A.; Jones, R. J.; Vaughan, R. W.; Kendrick, W. P. *NASA CR 72633*, **1970**.
(6) Wong, A. C.; Garroway, A. C.; Ritchey, W. M. *Macromolecules* **1981**, *14*, 832.
(7) Hay, J. N.; Boyle, J. D.; James, P. G.; Walter, J. R.; Wilson, D. *Polymer* **1989**, *30*, 1032.
(8) Bertholio, F.; Mison, P.; Pascal, T.; Sillion, B. *High Perform. Polym.* **1993**, *5*, 47.
(9) Ahn, M. K.; Stringfellow, T. C.; Fasano, M.; Bowles, K. J.; Meador, M. A. *J. Polym. Sci., Part B* **1993**, *31*, 831.
(10) Ahn, M. K.; Smirnov, A. I.; Smirnova, T. I.; Belford, R. L. *Macromolecules* **1995**, *28*, 7026.
(11) Jacob, G. S.; Schaefer, J.; Stejskal, E. O.; McKay, R. A. *J. Biol. Chem.* **1987**, *260*, 5899.
(12) Afeworki, M.; McKay, R.; Schaefer, J. *Macromolecules*, **1992**, *25*, 4084.
(13) Stejskal, E. O.; Schaefer, J.; Sefcik, M. D.; McKay, R. A. *Macromolecules* **1981**, *14*, 275.
(14) Kuroda, Shin ichi; Mita, Itaru *Eur. Polym.* **1989**, *25*, 611.
(15) George, M. A.; Ramakrishna, B. L.; Glausinger, W. S. *J. Phys. Chem.* **1990**, *94*, 5159.
(16) Wind, R. A.; Duijvestijn, M. J.; Van Der Lugt, C.; Manenschijn, A.; Vriend, J. *Prog. NMR Spectrosc.* **1985**, *17*, 33.
(17) Wertz, J. E.; Bolton, J. R. *Electron Spin Resonance Elementary Theory and Practical Applications*; McGraw Hill: New York, **1986**.
(18) Boer, E. de; van Willigen, H. *Prog. NMR Spectrosc.* **1967**, *2*, 111.

MA961480A